

RESEARCH ARTICLE

Evolutionarily conserved primary TNF sequences relate to its primitive functions in cell death induction

Wenshu Lu^{1,*}, Qiongyu Chen^{1,*}, Songmin Ying¹, Xiaobing Xia¹, Zhanru Yu², Yuan Lui², George Tranter³, Boquan Jin⁴, Chaojun Song⁴, Leonard W. Seymour^{1,‡} and Shisong Jiang^{1,‡}

ABSTRACT

TNF is a primitive protein that has emerged from more than 550 million years of evolution. Our bioinformatics study of TNF from nine different taxa in vertebrates revealed several conserved regions in the TNF sequence. By screening overlapping peptides derived from human TNF to determine their role in three different TNF-induced processes – apoptosis, necrosis and NF- κ B stimulation – we found that TNF conserved regions are mostly related to cell death rather than NF- κ B stimulation. Among the most conserved regions, peptides (P)12, P13 and P1213 (comprising P12 and P13) induced apoptosis, whereas P14, P15, P16 and P1516 (comprising P15 and P16) induced necrosis. Cell death induced by these peptides was not through binding to the TNF receptor. P16-induced necrosis was mainly through disruption of the cell membrane, whereas P1213-induced apoptosis involved activation of TRADD followed by formation of complex II. Finally, using a monoclonal antibody and a mutant TNF protein, we show that TNF-induced apoptosis is determined by a conserved linear sequence that corresponds to that within P1213. Our results reveal the determinant sequence that is key to the TNF primitive function of inducing apoptosis.

KEY WORDS: TNF, NF- κ B, Apoptosis, Necrosis, Evolution, Overlapping peptides

INTRODUCTION

Tumor necrosis factor (TNF) is a multifunctional cytokine that is secreted by various cells, but mainly macrophages and T cells. TNF is thought to have emerged during the Precambrian era (more than 550 million years ago) before the animal phyla started to evolve (Quistad et al., 2014). The fact that certain functions of TNF – e.g. induction of cell death – have remained unchanged during the process of evolution indicates that some parts of the TNF structure, either primary or conformational, are probably conserved between different species.

TNF has two forms, a 26-kDa membrane form and a 17-kDa soluble form. The latter is formed through enzymatic cleavage of the membrane form by a TNF-converting enzyme (TCE). TNF performs functions as a trimer, which then binds to one of its two

receptors, the 55-kDa TNF receptor 1 (TNFR1; also known as TNFRSF1A) or the 75-kDa TNF receptor 2 (TNFR2; also known as TNFRSF1B). TNFR1 exists constitutively on most cell surfaces and functions when activated by trimerized TNF. TNFR2 is expressed, in a highly regulated way, on the surface of several cell types, such as immune cells, endothelial cells, epithelial cells and neuronal cells (Martin et al., 2014). Activation of TNFR2 leads to signal pathways that are different to that of TNFR1 (Hehlhans and Pfeffer, 2005). TNF induces multiple biological functions, and many of these follow from three major intracellular events: (1) stimulation of the transcription factor nuclear factor kappa B (NF- κ B), leading to cell activation and cytokine production; (2) induction of the extrinsic pathway of cell apoptosis (Declercq et al., 2009; Galluzzi and Kroemer, 2008; Hitomi et al., 2008); and (3) induction of necrosis. In some situations, it has been reported that inhibition of caspases during apoptosis can lead to a form of programmed cell death that can occur with features of necrosis, termed ‘necroptosis’ (Berghe et al., 2010; Chan et al., 2003; Declercq et al., 2009; Galluzzi and Kroemer, 2008; Hitomi et al., 2008; Vandenabeele et al., 2010).

Many reports have explored the mechanism of TNF multifunctionality by studying its signal transduction pathways (Declercq et al., 2009). In most cases, stimulating cells with TNF primarily activates NF- κ B to promote cell survival (Fig. S1). Apoptosis and necrosis are only triggered when the NF- κ B pathway is inhibited (Varfolomeev and Ashkenazi, 2004). It has been proposed that TNF stimulates a membrane-bound complex (complex I), which includes the following components: TNFR1, TNF-receptor-associated death domain (TRADD), the receptor-interacting protein kinase 1 (RIP1), TNF-receptor-associated factor 2 (TRAF2) and cellular inhibitor of apoptosis 1 and 2 (c-IAP1 and c-IAP2, respectively) (Micheau and Tschopp, 2003). Complex I initiates NF- κ B activation but not apoptosis and/or necrosis. However, if NF- κ B activation is absent, TNF stimulates its target cells to form a second complex (complex II) in the cytoplasm, which compared to complex I, lacks TNFR1 and c-IAP1 but includes Fas-associated death domain (FADD), caspase-8 and caspase-10. Complex II then triggers apoptosis and/or necrosis (Fig. S1). RIP1 has been thought to be important in the activation of NF- κ B, but its role has been recently challenged by the observation that NF- κ B activation can occur independently of RIP1 (Wong et al., 2010). Moreover, another RIP-family member in complex II, RIP3, has been shown to be crucial in the cell death process. RIP3 induces a death signal that leads to necrosis (necroptosis) when caspase-8 is inhibited (He et al., 2009; Zhang et al., 2009) (Fig. S1).

Although the mechanism of how intracellular signals are transduced after TNF–TNFR1 binding is now well characterized, the study of the target cells alone has not so far created any clinically valued opportunity for intervention of TNF related pathogenesis. By contrast, blocking TNF with monoclonal antibodies or soluble TNFR2 (Etanercept) has generated great benefit for patients

¹Department of Oncology, University of Oxford, Old Road Campus Research Building, Roosevelt Drive, Oxford OX3 7DQ, UK. ²MRC Immunology Unit, Weatherall Institute of Molecular Medicine, University of Oxford, John Radcliffe Hospital, Headington OX3 9DS, UK. ³Chiralabs Limited, Begbroke Science Park, Woodstock Road, Begbroke, Oxfordshire OX5 1PF, UK. ⁴Department of Immunology, Fourth Military Medical University, Xi'an City 710032, Shaanxi Province, China.

*These authors contributed equally to this work

‡Authors for correspondence (len.seymour@oncology.ox.ac.uk; shisong.jiang@oncology.ox.ac.uk)

(Feldmann, 2009), indicating the importance of investigating the ligand itself. Nevertheless, the role that the TNF primary sequence plays in its various functions has not been widely studied. For example, do distinct parts of the TNF molecule play a role in stimulating different functions? It is widely believed that evolutionarily conserved sequences in a protein are often of functional importance. Some amino acid sequences of TNF might remain unchanged in different species, but any correlation between the conserved sequences and the functions has yet to be established. Identification of these functional ‘footprints’ does not only help us to understand how TNF evolved but also provides potential biomarkers for intervention of TNF-related diseases.

As a result, this study sought to compare TNF sequences from different species to identify conserved sequences. Next, in order to identify whether the conserved sequences correlate with particular functions of TNF, we made a series of overlapping 20-mer peptides comprising the full-length of the membrane form of TNF. The ability of these peptides to mediate three distinct pharmacological outcomes (NF- κ B stimulation, apoptosis and necrosis) was measured using a series of cell lines, but mainly the Jurkat A3 T-cell line and the mouse fibrosarcoma L929 cells. Some of the peptides mediated strong pro-apoptotic and pro-necrotic mechanisms, and these were studied in detail. Inducing the inflammation-inhibitory process of apoptosis is one of the most important functions of TNF, and is a gateway leading to other forms of cell death – e.g. inflammatory necroptosis. Therefore, we investigated whether the apoptotic function of specific TNF peptides correlates with the function of the whole TNF molecule.

RESULTS

Most regions of TNF that are conserved across different vertebrates correlate with cell death

Conservation of protein sequence often serves as evidence for cellular functionality (Bejerano et al., 2004; Ghosh et al., 1998). TNF exists in different species within the vertebrate subphylum (Baena et al., 2007; Wiens and Glenney, 2011).

We therefore compared the TNF protein sequences in nine genetically diverse species (monkey, human, whale, mouse, sea turtle, lizard, fish, frog and shark) in the vertebrate subphylum. Fig. 1A shows a multiple sequence alignment of whole TNF sequences from the nine species (Fig. 1A). There are several conserved regions, which are marked by horizontal colored bars above the TNF sequences in Fig. 1A. These conserved regions are also shown in the TNF crystal structure (Eck and Sprang, 1989) in Fig. 1B (using the same colors as in Fig. 1A). The black lines and designation P1–P22 above the sequences in Fig. 1A indicate the overlapping peptides of the human TNF sequence that were made in order to screen for TNF-like activities. Fig. 1C shows a cytotoxicity assay using the overlapping TNF-derived peptides. The colors used in Fig. 1C represent the same conserved regions shown in Fig. 1A,B, and it is interesting that the peptides inducing the greatest cytotoxicity are those containing evolutionarily conserved sequences.

The conserved region shown in gray is located in overlapping peptides P3 and P4 (Fig. 1A). Because this region represents the trans-membrane domain of TNF, it is not shown in the crystal structure of soluble TNF. Both P3 and P4 were found to be cytotoxic (Fig. 1C). The conserved region in red partly comprises P12 and P13 (Fig. 1A). This region includes two β -strands that are connected by a loop and is located at the exterior surface of the trimeric TNF crystal structure (Fig. 1B). Overlapping peptides comprising this region are also cytotoxic (Fig. 1C). The conserved regions in orange, green and

purple relate to P13–P16, P19–P20 and P22, respectively. All these conserved sequences are hidden at the trimer-interface side of the TNF crystal structure (Fig. 1B); however, the peptides derived from these regions are all cytotoxic (Fig. 1C). The conserved region in yellow is comprised by the sequences of P16–P18 (mainly P17–P18) (Fig. 1A), and the region is mainly located at the external surface of the trimeric TNF crystal structure (Fig. 1B). Interestingly, although P16 induces cytotoxicity, P17 and P18 contain conserved regions without obvious cytotoxic effects (Fig. 1C).

Peptides containing conserved sequences induce apoptosis as well as non-programmed necrosis in Jurkat A3 cells and L929 cells

To investigate systematically whether the TNF conserved sequences (vs non-conserved sequences) mediate special cellular functions, overlapping synthetic peptides corresponding to the human TNF sequence were screened in an NF- κ B assay, and in a high-throughput flow-cytometry-based screen for induction of apoptosis and necrosis. The overlapping synthetic peptides were designed as a series of linear 20-amino-acid peptides, P1–P22, the sequences of which comprised the complete length of the membrane form (or ‘pro-form’) of TNF (amino acids 1–233) (http://www.uniprot.org/uniprot/NP_000585.2). Each peptide sequence overlapped the adjacent peptides by 10 amino acids, and the C-terminal peptide was 23 amino acids in length (Fig. 1A). We used the assays to screen whether the peptides could mediate the major functions of TNF, including activation of NF- κ B and induction of cell death (apoptosis and/or necrosis).

Several peptides showed activities of inducing cell death. As mentioned above, cell-death-inducing peptides largely coincided with conserved sequences (Fig. 1). In this article, we focused on the series of peptides P12–P16, as these sequences comprised the most conserved sequences of TNF (Fig. 1A). Moreover, these peptides are consecutively linked in tandem but can be divided functionally into two groups; in both Jurkat A3 and L929 cells, P12 and P13 induced mainly apoptosis, and P14–P16 induced mainly necrosis (Fig. 2A,B). Peptide P18 never induced cell death and was therefore used as a negative control.

Within the region covered by P12–P13, there was a slight sequence variation for induction of apoptosis between Jurkat A3 and L929 cells; both P12 and P13 induced strong apoptosis in Jurkat A3 cells (Fig. 2A–C), whereas only P13 induced apoptosis in L929 cells (Fig. 2B). For the induction of necrosis, P14, P15 and P16 induced strong necrosis in both Jurkat A3 and L929 cells (Fig. 2A,B).

z-VAD-fluoromethylketone (z-VAD-FMK or z-VAD) is a specific caspase inhibitor (Van Noorden, 2001). A combination of TNF and z-VAD has been reported to induce regulated necrosis or necroptosis in L929 cells (Hitomi et al., 2008; Vercammen et al., 1998; Wu et al., 2011). We found a similar phenomenon in Jurkat A3 T cells when apoptosis was mediated by the TNF peptides. The apoptosis in Jurkat A3 cells that was induced by these peptides could be inhibited with z-VAD (Fig. 2C). P12- and P13- induced apoptosis in Jurkat A3 cells was converted into partially live cells and partially regulated necrosis after addition of z-VAD (Fig. 2C).

Because the peptide sequence varied slightly between cell lines, we made 30-mer-long peptides P1213 (comprising P12 and P13, P1213: ALLANGVELRDNQLVVPSEGLYLIYSQVLF; P12: ALLANGVELRDNQLVVP) and P1516 (comprising P15 and P16, P1516: KGQGPCSTHVLLTHTISRIVSYQTKVNLL; P15: KGQGPCSTHVLLTHTISRIV; P16: LLTHTISRIVSYQTKVNLL) – P1213 induced predominantly apoptosis, whereas P1516 induced necrosis in Jurkat A3 cells (Fig. 2D; Fig. S2B).

Fig. 1. TNF conserved sequences across nine vertebrate taxa, their position in the crystal structure and their relationship to induction of cell death. (A) Multiple TNF protein sequence alignment of frog (NP_001108250.1), fish (XP_006007247.1), human (NP_000585.2), monkey (NP_001040614.1), whale (Q8WNR1.1), mouse (NP_038721.1), sea turtle (XP_007053265.1), lizard (XP_008103955.1) and shark (AGQ17907.1). The amino acids that are 100% conserved are shaded in black and marked with an asterisk (*) underneath the shading. The gray shading and a colon (:) underneath indicate conservation between groups of strongly similar properties – scoring >0.5 in the Gonnet PAM 250 matrix (<http://www.ebi.ac.uk/Tools/msa/clustalo/help/faq.html#23>). The lighter gray shading and a period (.) underneath indicate conservation between groups of weakly similar properties – scoring ≤0.5 in the Gonnet PAM 250 matrix. Above the alignment, a series of overlapping peptides derived from the human TNF sequence (P1–P22) and the lengths of these peptides (lines after the names) is shown. The colored bars represent different regions of conserved sequences. (B) The position of the conserved sequences are shown in the corresponding colors in the crystal structure of TNF. (C) Jurkat A3 cell death induced by the human TNF overlapping peptides. The cell death shown represents the sum of apoptosis (measured using caspase-3 activation) and necrosis (live–dead staining). The concentration of the peptides is 50 μM. The colors correspond to the regions of conserved sequence shown in A,B. C shows a typical result from three replicate experiments. Mean±s.d. of three experiments are shown. No, no peptide.

necrosis (Fig. S2B), suggesting that P1516-induced necrosis might not be necroptosis.

Cell death was further confirmed with fluorescence microscopy analyses. DNA fragmentation during peptide-induced apoptosis, as visualized with DAPI staining, coincided with expression of active caspase-3 (Fig. 2E). These experiments suggest that P12-induced apoptosis in Jurkat A3 cells might be converted into programmed necrosis in the presence of caspase inhibitors, and this feature has been defined as necroptosis (Galluzzi and Kroemer, 2008).

We also investigated the cell death by using transmission electron microscopy. P12- and P13-treated Jurkat A3 cells showed condensation and fragmentation of nuclei and blebbing; P15- and P16-treated cells showed disintegration of the cell membrane, swelling of organelles and release of intracellular contents (Fig. 2F).

Soluble TNF activated NF-κB in Jurkat A3 T cells at concentrations as low as 0.5–1 nM (Fig. S3A). However, we observed that, in Jurkat A3 T cells, none of the peptides were able to activate NF-κB, even at concentrations of 100 μM (Fig. S3B). At 1 min after treatment, there was no significant NF-κB activation in either TNF- or peptide-treated cells. At 5 min, only TNF stimulated NF-κB. This result indicates that the peptides have different NF-κB-stimulation kinetics compared with TNF. The peptides did not show NF-κB stimulation activity at any of the multiple time points or doses tested (Fig. S3B,C). Peptides P11–P18 were also tested with a NF-κB reporter cell line (THP-1 human monocyte) and showed no activation of NF-κB across a broad concentration range (Fig. S3C). These results suggest that either the NF-κB activation process requires involvement of more than one TNF peptide chain, for example the ability to trimerize, or that it requires conformational properties of the TNF molecule that are lost in the peptide fragments.

Cell death induced by peptides is independent of TNFR1

We firstly tested whether P1213 and P16 bound to TNFR1 by using immunofluorescence staining, which can be observed with a confocal microscope. Staining the peptides and TNFR1 in Saos-2 (human Osteosarcoma) cells showed no colocalization between the peptides and TNFR1. Only TNF (positive control) was found to colocalize with TNFR1 (Fig. 3A). This result indicates that, unlike the whole molecule of TNF, the functioning peptides do not bind to TNFR1. This result was further confirmed by using a TRADD immunoprecipitation assay in Jurkat A3 cells. TRADD is a key

intracellular protein that serves as a scaffold to attract various proteins to form either complex I or complex II in order to initiate different TNF functions. We therefore tried to immunoprecipitate TRADD after peptide and/or TNF stimulation. TNFR1 could be co-precipitated with TRADD after TNF stimulation, whereas it could not be co-immunoprecipitated with TRADD after stimulation with P1213 (Fig. 3B). The receptor-binding ability of the peptides was also assessed with an ELISA assay in which ELISA plates were coated with avidin, followed by the addition of biotinylated peptides (biotinylation did not affect the pro-apoptotic function of P1213; see Fig. S4A). Next, the plates were incubated with TNFR1 before detection with an antibody against TNFR1 and a second antibody conjugated with horseradish peroxidase (HRP). As Fig. S4B shows, none of the peptides tested was able to bind to TNFR1. Binding of TNFR1 and TNFR2 to TNF, P1213 or P16 was also tested using Biacore surface plasmon resonance analysis. As shown in Fig. S4C, only TNF bound to both TNFR1 and TNFR2. Neither P1213 nor P16 bound to TNF receptors (Fig. S4C). We also tested whether blocking TNFR1 with a neutralizing monoclonal antibody against TNFR1 would inhibit P1213- or TNF-induced apoptosis. As Fig. 3C shows, blocking TNFR1 only inhibited TNF-induced apoptosis in L929 cells and not P1213-induced apoptosis (Fig. 3C). Lastly, we tested whether P1213 induces apoptosis in Jurkat A3 cells in which TNFR1 had been knocked down with small interfering (si)RNAs. As shown in Fig. 3D, after knockdown of TNFR1, the TNFR1 expression level was highly reduced (right panel), but apoptosis was induced no matter whether TNFR1 was inhibited or not (Fig. 3D, left panel). These data suggest that TNFR1 is not required for peptide-related apoptosis or necrosis.

Apoptosis induced by P1213 involves formation of complex II, comprising TRADD, RIP1, caspase-8 and FADD

To study the signal pathway of peptide-induced apoptosis, we focused on P1213-induced apoptosis. Although P1213-induced apoptosis was independent of TNFR1 (Fig. 3), the fact that it stimulated activation of caspase-3 (apoptosis was assayed by measuring active caspase-3; Fig. 3D) hints that the intracellular signals must be involved in the process. To examine this, we first checked whether P1213 enters cells. We performed an experiment in which we incubated P1213-biotin with HT29 cells (chosen because their membrane can be clearly stained with an antibody against E-cadherin) for 2 h at 37°C, and stained P1213 and the cell membrane. We used a confocal microscope to observe the position of P1213 in relation to the cell membrane. As shown in Fig. 4A, P1213 (green) was found in different confocal-section layers on the cell membrane (red) and within the cell.

We then investigated whether P1213 colocalized with TRADD in Saos-2 cells. As shown in Fig. 4B, colocalization was seen as early as incubating P1213 and Saos-2 cells for 10 min, suggesting that binding of the peptide to TRADD is an early event.

Next, by immunoprecipitating TRADD from Jurkat A3 cells, we found that after 2 h of stimulation with TNF, both RIP1 and FADD could be co-immunoprecipitated upon exposure of cells to P1213 (Fig. 4C), implying that a complex (most likely complex II) was formed, comprising at least TRADD, RIP1 and FADD. The nonspecific bands seen either side of the RIP1 signal relate to the 50-kDa and 100-kDa monomer and dimer heavy chains, respectively, of the antibody against TRADD, which are recognized by the anti-mouse secondary antibody. Finally, we employed Jurkat-A3-based knockout cell lines – Jurkat RIP (RIP1^{-/-}), I9.2 (caspase-8^{-/-}) and I2.1 (FADD^{-/-}). Apoptosis induced by P1213 was significantly

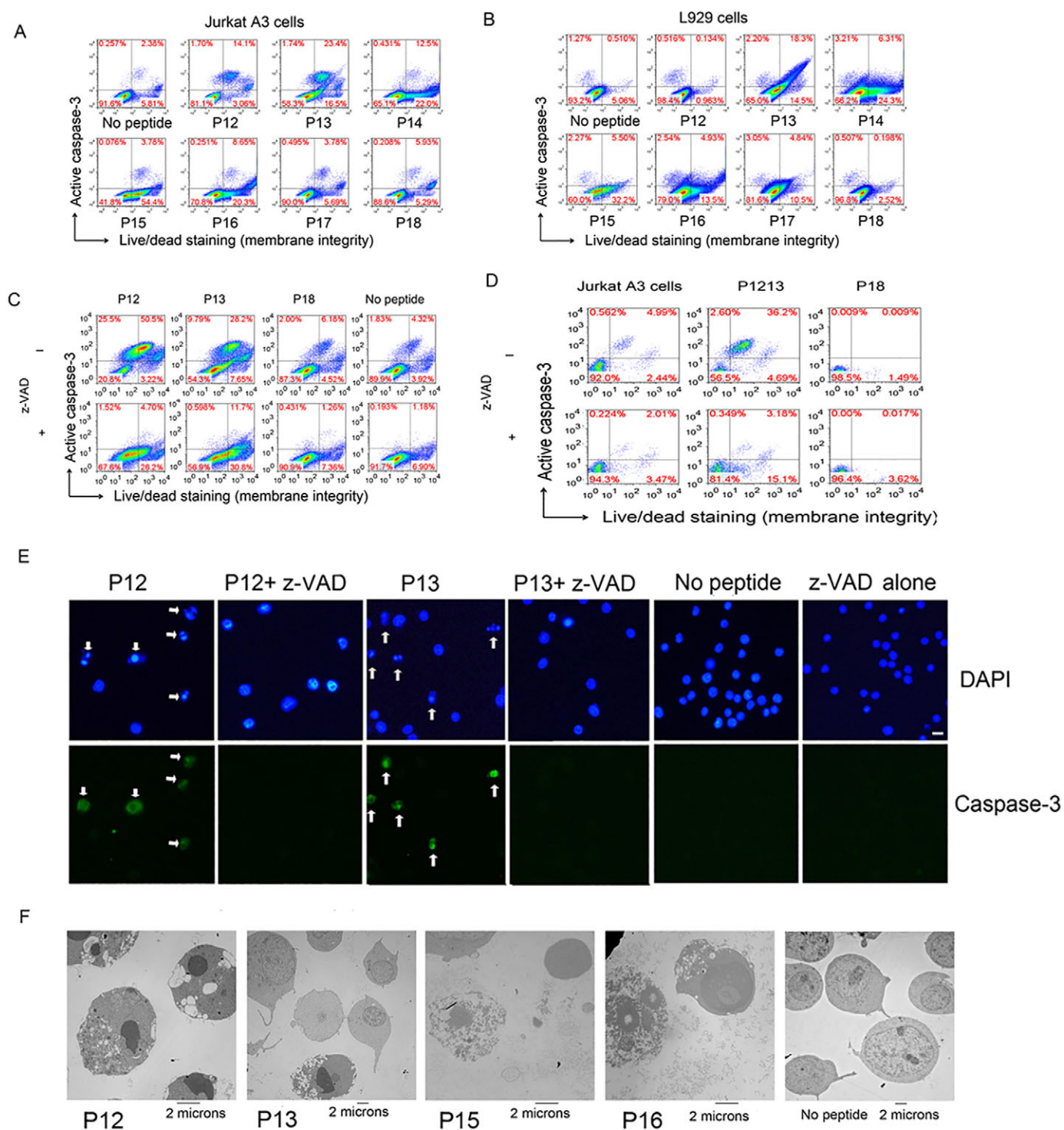


Fig. 2. Screening and characterizing TNF peptides for the induction of apoptosis and necrosis. (A,B) Cell death induced by selected 20-mer TNF peptides (P12–P18). Each of the overlapping peptides was incubated overnight at 50 μ M with Jurkat A3 (A) or L929 (B) cells. Apoptosis and necrosis were measured by using flow cytometry analysis of active caspase-3 and membrane integrity (live–dead cell staining), respectively. The experiments were repeated more than five times. (C) z-VAD inhibited peptide-induced apoptosis. Jurkat A3 cells were incubated overnight with 100 μ M of P12, P13 and P18, in the presence of 10 μ M z-VAD. The experiment was repeated three times. (D) Apoptosis induced by the 30-mer peptide P1213. Jurkat A3 cells were incubated with the 30-mer peptide P1213 at 30 μ M overnight, with or without the presence of 10 μ M z-VAD. P18 was used as a control peptide. The experiment was repeated three times. (E) DNA fragmentation coincided with active caspase-3 expression in P12- and P13-induced apoptosis. P12- and P13-induced apoptosis is shown in fluorescence images of DAPI-stained nuclei with DNA fragmentation (upper panel) and fluorescence-labeled active caspase-3 (lower panel). White arrows point to nuclear DNA fragmentation (upper panel), which coincides with caspase-3 activation in the cells without z-VAD (lower panel). Scale bar: 20 μ m. The experiment was repeated twice. (F) Transmission electron microscopy analysis of TNF-peptide-treated cells. Jurkat A3 cells were treated with selected peptides (P12, P13, P15 and P16) at 100 μ M. Cells cultured with P12 and P13 show DNA fragmentation, blebbing and membrane shedding, whereas cells treated with P15 and P16 show necrosis-like features, such as loss of cell membrane integrity.

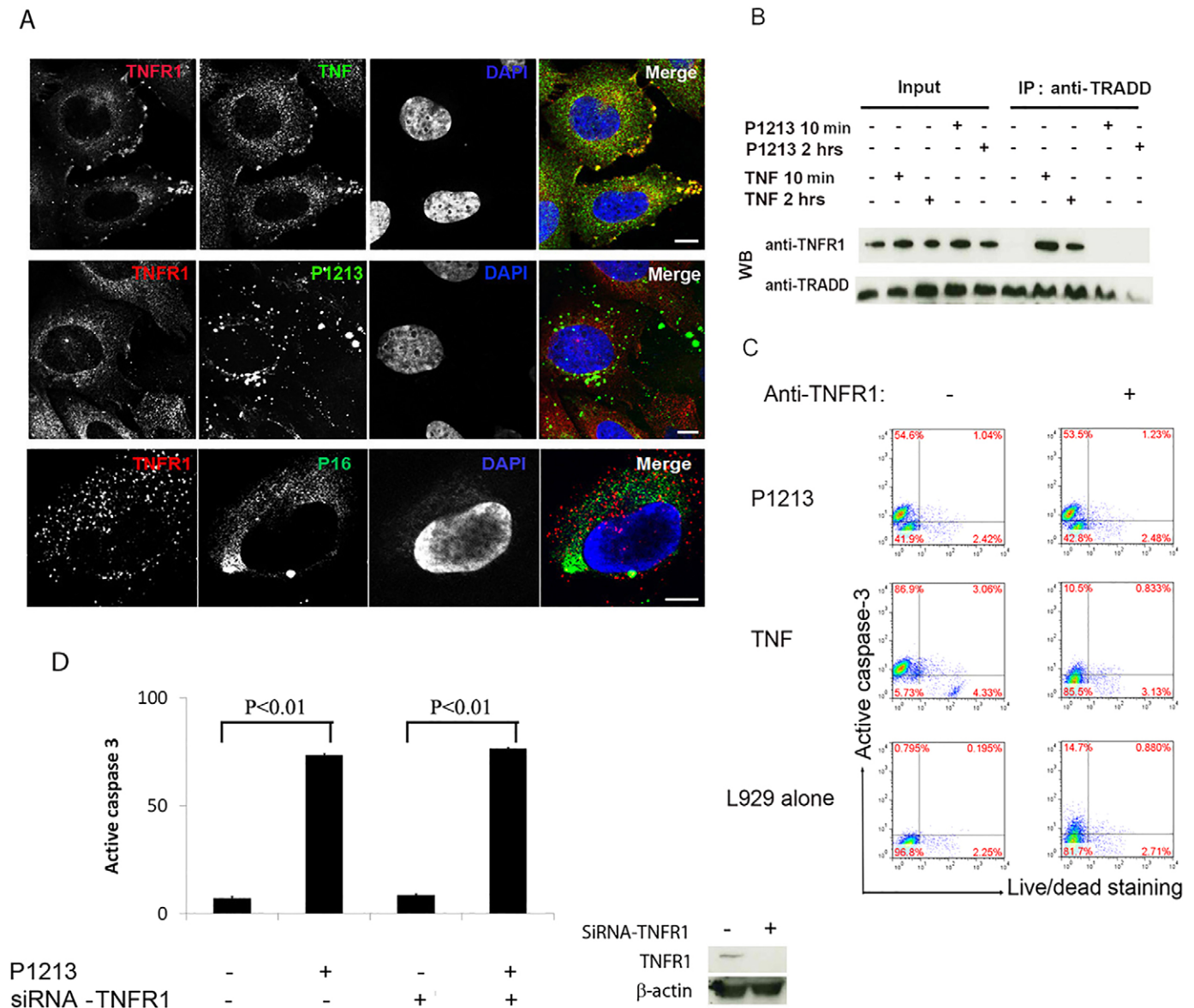


Fig. 3. Cell death induced by peptides is independent of TNFR1. (A) Confocal microscopy images showing that the peptides do not bind to TNFR1. Biotinylated P1213 or P16 were incubated with Jurkat A3 cells; biotinylated TNF was used as a positive control. After incubation with cells, peptides or TNF were stained with avidin conjugated with Alexa-Fluor-488. TNFR1 was stained with an antibody against TNFR1, followed by a second antibody conjugated with Alexa-Fluor-568. Scale bar: 10 μ m. (B) P1213 does not cause TNFR1 to co-immunoprecipitate with TRADD. Jurkat A3 cells stimulated with P1213 or TNF at the indicated times were subjected to immunoprecipitation (IP) with an antibody against TRADD, followed by western blotting (WB) for TNFR1. (C) L929 cells were incubated with 20 ng/ml TNF or 50 μ M P1213 in the presence or absence of an antibody against TNFR1 (Anti-TNFR1; 20 μ g/ml) overnight. (D) Functionally, P1213-induced apoptosis is independent of siRNA-mediated TNFR1 (siRNA-TNFR1) inhibition. Jurkat A3 cells that had been treated with or without siRNA-TNFR1 were incubated with P1213, and active caspase-3 in the cells was then measured. The right-hand panel shows inhibition of TNFR1 expression after siRNA-TNFR1 treatment by western blotting. All experiments were repeated at least twice. Means \pm s.d. of triplicate experiments are shown. *P*-values were calculated using Student's *t*-test.

reduced in all three cell lines compared to that in wild-type Jurkat A3 cells ($P < 0.05$; Fig. 4D), suggesting that a key role is played by these proteins. All these results indicate that the signaling pathway of peptide-induced apoptosis is similar to that of TNF, except for the exclusion of TNFR1. Peptide-induced apoptosis could be initiated through direct binding to TRADD, followed by formation of complex II.

Necrosis induced by P16 is due to direct disruption of the cell membrane

When using circular dichroism to examine whether any of the TNF peptides retained any structural configuration, the circular

dichroism of P15 and P16 stood out as being of a substantially less-negative (lower) magnitude of ~ 190 – 200 nm when compared with that of P18 (used as a control peptide), and of a proportionately greater magnitude of ~ 210 – 220 nm. The particular form of the circular dichroism spectra suggests that P15 and P16 contain a somewhat greater proportion of β -sheet structure (Fig. 5A) (Greenfield, 2007). The circular dichroism of P12 and of most other peptides, however, was similar to that of the control peptide P18 (data not shown).

Interestingly, when incubating P16 with differently charged lipid vesicles, the circular dichroism spectrum of P16 in the negative-charged

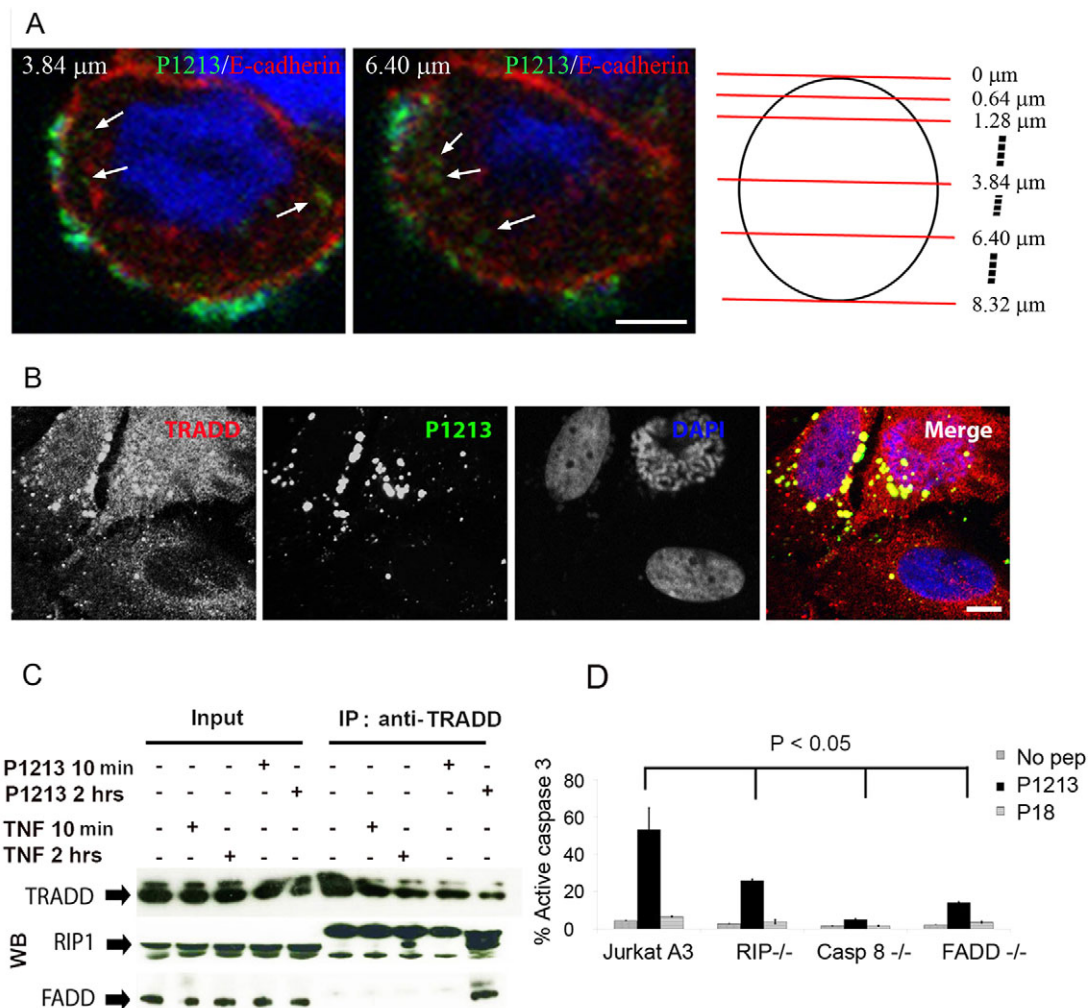


Fig. 4. P1213 enters cells and stimulates apoptotic complex-II formation. (A) P1213 enters cells. HT29 cells were treated with P1213 for 2 h before fixation. The cells were incubated with an antibody against E-cadherin (to label the membrane) and further stained with a secondary antibody conjugated to Alexa-Fluor-568. The biotinylated P1213 was stained with avidin-conjugated Alexa-Fluor-488. The confocal images (left and middle panels), representing two different layers of cells at 3.84- μm and 6.40- μm sections scanning from top, show that P1213 (green) is located both on the cell membrane and within the intracellular compartment. The right panel is a schematic picture showing different layers scanned from top of the cells with the confocal microscope. The distance between each layer is 0.64 μm . (B) P1213 binds to TRADD. Jurkat A3 cells that had been stimulated with biotinylated P1213 were stained with avidin–Alexa-Fluor-488 and an antibody against TRADD, and were then subjected to confocal microscopy. Scale bar: 10 μm . (C) P1213 co-immunoprecipitates TRADD with RIP1 or with FADD. Jurkat A3 cells that had been stimulated with P1213 or TNF for the indicated times were subjected to immunoprecipitation (IP) with an antibody against TRADD, followed by western blotting (WB) for RIP1 or FADD. The experiment was repeated twice. (D) P1213 does not induce apoptosis in RIP1^{-/-}, caspase-8^{-/-} or FADD^{-/-} cell lines. Jurkat A3 and Jurkat-A3-based knockout cell lines RIP^{-/-}, I9.2 (caspase-8^{-/-}) and I2.1 (FADD^{-/-}) were incubated with P1213 overnight, followed by measurement of intracellular active caspase-3. The error bars represent mean \pm s.d. of three experiments. *P*-values were calculated using Student's *t* test. No pep, no peptide.

lipid vesicles [palmitoyl-oleoyl-phosphatidylcholine and palmitoyl-oleoyl-phosphatidylserine (POPC:POPS) bilayers] showed a more negative signal at 220 nm (Fig. 5B), with a typical α -helix profile (Greenfield, 2007), indicating that the structure of P16 might have been changed by the negatively charged lipid membrane (Fig. 5B).

Dynamic light scattering analyses of P16 revealed that the size of the peptide increased more than three times when changed from a hydrophilic environment to a hydrophobic one (Fig. 5C,D), indicating that P16 aggregates in the hydrophobic environment.

Based on these observations and the fact that P16-related necrosis appears to be independent of TNFR1, we suspected that the peptide might interact directly with the cell membrane, perhaps reflecting charge interactions. To assess this, we incubated P16 and P12 with

human red blood cells (RBCs), which have a negatively charged membrane but no TNFRs nor intracellular organelles (Fernandes et al., 2011). After overnight culture, the membranes of the RBCs that had been incubated with P16 were ruptured, and hemoglobin was released into the supernatant (Fig. 5E,F). Disruption of the lipid membrane was further shown by incubation of P16 with liposomes that contained a fluorophore (Phen Green SK). Again, the liposome of the negatively charged membrane (POPC:POPS) showed more susceptibility to P16-mediated damage (Fig. 5G). Thus, it appears that the necrosis induced by (cationic) P16 might be due to direct damage to the cell membrane as a result of membrane-mediated structure change and aggregation. Moreover, P16-induced necrosis reflects a different mechanism from the necroptosis induced by P12 or P1213 in the presence of z-VAD.

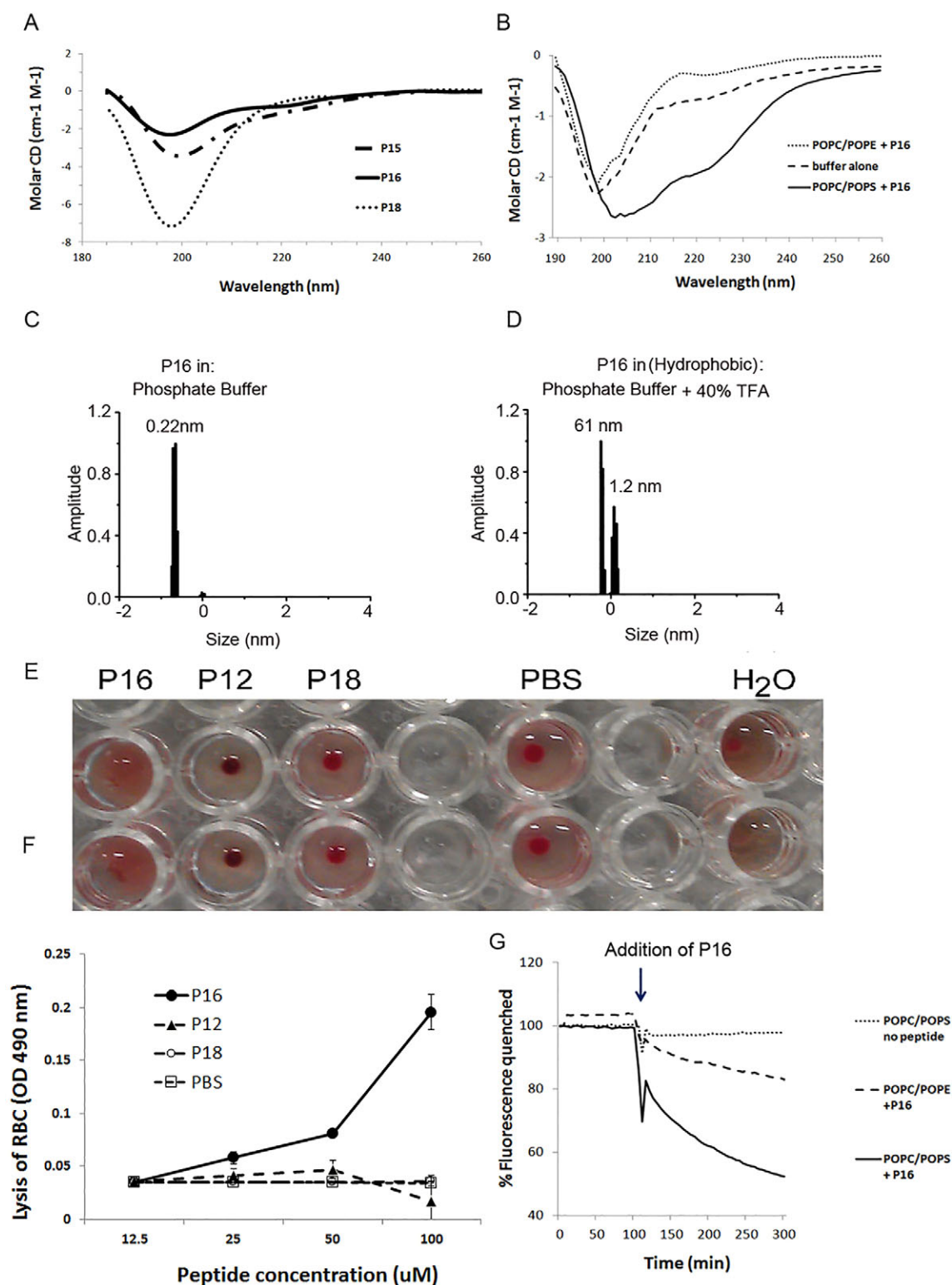


Fig. 5. Membrane-induced P16 structural changes, aggregation and membrane disruption. (A) Molar circular dichroism spectra of selected peptides at pH 7.4 (normalized for the number of peptide linkages). The circular dichroism spectra of P15, P16 and P18 are shown. (B) Circular dichroism spectra of P16 (50 μM) in aqueous buffer solution (thick dotted line), neutral POPC:POPE liposomes (thin dotted line) or negatively charged POPC:POPS liposomes (solid line). (C,D) Hydrodynamic radius (nm) of P16 measured using dynamic light scattering in (C) hydrophilic conditions or (D) hydrophobic conditions. (E) P16 disrupts cell membranes of RBCs. RBCs ($10^7/100 \mu\text{l}$) were incubated with peptides at a concentration of 100 μM overnight. Lysis of RBCs by P16 or H₂O was observed, but not by P12, P18 or PBS. (F) P16 disrupts cell membranes of RBCs. RBCs ($10^7/100 \mu\text{l}$) were incubated with different concentrations of peptides overnight. Protein (mainly hemoglobin) in the supernatant was measured to indicate cell lysis. The experiments were repeated three times. (G) P16 (50 μM) was incubated with negatively charged POPC:POPS liposomes or pH-neutral POPC:POPE liposomes encapsulating a fluorescent marker (Phen Green SK). Disruption of the membrane was measured by the quenching of fluorescence intensity inside liposomes (fluorescence decreased, arrow). The error bars represent mean \pm s.d. of three experiments.

P1213 is key to TNF-induced apoptosis

Results presented above characterize the function of the P1213 peptide, which might be different from that of the whole TNF molecule. To study whether the P1213 sequence in the whole TNF molecule remains functional and is responsible for the apoptosis-inducing function of the whole TNF molecule, we produced 33 monoclonal antibodies (mAbs) by immunizing mice with P1213, with a view to trying to block P1213-induced apoptosis. One precondition of this study was that the mAb should bind to TNF but not interfere with the binding of TNF to its receptor. Five of these mAbs were able to bind to intact TNF (Fig. 6A), and we selected mAb 244-12, which exhibited the strongest binding to TNF, for further study.

First, we investigated the binding epitope of mAb 244-12 by screening a series of 10-mer overlapping peptides. These peptides overlapped the sequence of their adjacent peptides by nine amino acids on each side (Fig. 6B), and they comprised the whole sequence of P1213. We employed an ELISA assay that measured the binding of mAb 244-12 to TNF in order to determine whether the binding could be inhibited by individual 10-mer peptides. Inhibition of mAb 244-12 binding to TNF in the presence of any 10-mer peptide meant that the epitope existed in the peptide. As shown in Fig. 6C, four consecutive peptides significantly inhibited the binding of mAb 244-12 to TNF. The common sequence of these four peptides is QLVVPSE. Therefore, the binding epitope of mAb 244-12 to TNF includes QLVVPSE (Fig. 6B,C).

We engineered a mutant TNF protein (mTNF-HA) in which the sequence QLVVPSE was replaced with the human influenza hemagglutinin (HA) tag (YPYDVPDYA) (Fig. 6D, upper panel). Functionally, unlike native TNF, expression of mTNF-HA did not kill L929 cells (Fig. 6D, lower panel) in the Crystal-Violet-based TNF cytotoxicity assay (Hogan and Vogel, 2001). On the contrary, it inhibited the killing of L929 cells that was induced by wild-type TNF (Fig. 6D, lower panel), suggesting a mechanism of receptor-competition and inhibition for mTNF-HA. This also suggests that mTNF-HA might have a similar conformational structure to that of wild-type TNF, which allows it to compete. To confirm that mTNF-HA binds to TNFR1, we performed an ELISA assay, which showed strong binding activity (Fig. S4D).

Next we examined whether binding of mAb 244-12 to TNF interferes with the binding of TNF to TNFR1 on the surface of L929 cells. As shown in Fig. 6E, mAb 244-12 colocalized with TNFR1 only in the presence of TNF, suggesting that binding of mAb 244-12 to TNF does not affect TNF binding to TNFR1 (Fig. 6E).

Finally, we examined whether binding of mAb 244-12 to TNF blocks TNF-induced apoptosis. Two cell lines, L929 and C28I2 (a human chondrocyte cell line) were employed in the study. As Fig. 6F shows, in both cell lines, adding mAb 244-12 to TNF-stimulated cells significantly inhibited activation of caspase-3 compared to that without the mAb ($P < 0.01$ and $P < 0.05$ for L929 and C28I2 cells, respectively). It was also noted that co-culture of mTNF-HA with L929 cells instead of wild-type TNF also eliminated induction of apoptosis. These data suggest that the region of TNF that corresponds to the sequence of P1213 is key to the apoptosis-inducing function of TNF.

DISCUSSION

The central scientific questions to be addressed in this study were whether there are any genetically conserved sequences in the primitive and multi-functional protein TNF, and whether any such sequences are involved in important conserved TNF functions?

By aligning the TNF sequences of different species, we discovered several genetically conserved regions (Fig. 1). Surprisingly, we

found that most of these regions appear to be linked with the TNF function of inducing cell death (Figs 1C and 2), but not stimulation of cell proliferation (Fig. S3). Accordingly, it might be that induction of cell death requires only a linear sequence, whereas stimulation of proliferation could require a higher-level structure of TNF.

We sought to explain our discovery from the aspect of TNF evolution. TNF has evolved to be very important in both innate and adaptive immunity. As Quistad et al. have reported, the origin of TNF can be dated back to 550 million years ago, well before the divergence of vertebrates and invertebrates (Quistad et al., 2014). Our data suggest that the highly conserved regions of TNF structure are those that play a role in cell toxicity, and it is possible that this was originally the sole molecular function. However, as evolution progressed, the molecule appears to have adapted and diverged between species, with new functions (such as stimulation of NF- κ B) developing and the sophisticated functions requiring TNF to have a higher-order structure.

Here, we have explored the mechanisms of cell death induced by these peptides. We chose P12 and P1213 for detailed study of peptide-induced apoptosis, and P16 and P1516 for necrosis. None of the peptides induce death through TNFR1 (Fig. 3). Although we do not exclude the possibility of P1213 binding to cell membrane receptors that directly activate TRADD to form complex II, it is likely that the apoptosis induced by P1213 in Jurkat cells is mediated by binding of the intracellular peptide to TRADD directly, followed by formation of complex II (RIP, caspase-8, FADD and caspase-3; Fig. 4). This process is independent of TNFR1 (Fig. 3).

Generally speaking, there are two mechanisms by which a peptide can enter cells: (1) in an energy-independent manner, such as internalization and diffusion; (2) through energy-dependent pathways, such as receptor-mediated entrance. By analyzing the sequence of P1213 (with online software from Genescript), we found it to be an acidic peptide (net charge of -2 ; isoelectric point of pH 3.69). Because most cell membranes are either electronically neutral (e.g. normal cells) or negatively charged (e.g. tumor cells) (Hilchie et al., 2011; Riedl et al., 2011), it is unlikely that the peptide crosses a cell membrane of the same electric charge using diffusion or an energy-independent pathway. Instead, energy will be required for the peptide to enter the cells. For example, the peptide might bind to a receptor (other than TNFR1), which helps the peptide to enter cells.

In summary, we have shown that P1213 probably enters the cell through an energy-dependent pathway (e.g. binding to a receptor) and that it then binds to TRADD to form complex II before initiating apoptosis.

P12- and P1213-induced apoptosis showed similar features to that induced by TNF in L929 cells in that it can be inhibited by z-VAD, which changes the mode of cell death from apoptosis to necroptosis (Fig. 2). By contrast, P16 and P1516 induce necrosis in a different manner to TNF in L929 cells treated with z-VAD – P16-related necrosis is independent of caspase inhibition (Fig. S3) and P16 does not bind to TNFR1 (Fig. 3); instead, P16 probably works through direct disruption of the cell membrane because it permeabilizes RBCs (Fig. 5E,F) and liposome membranes (Fig. 5G). Moreover, these observations all suggest that P16-induced necrosis is fundamentally different from TNF-induced necroptosis. The features of P16 are very similar to certain characteristics of cationic antimicrobial peptides (Peschel and Sahl, 2006), which are regarded a primitive defense mechanism. Notably, the P16 molecule, although very active in isolation, does not have any membrane-permeabilizing activity in the intact TNF molecule.

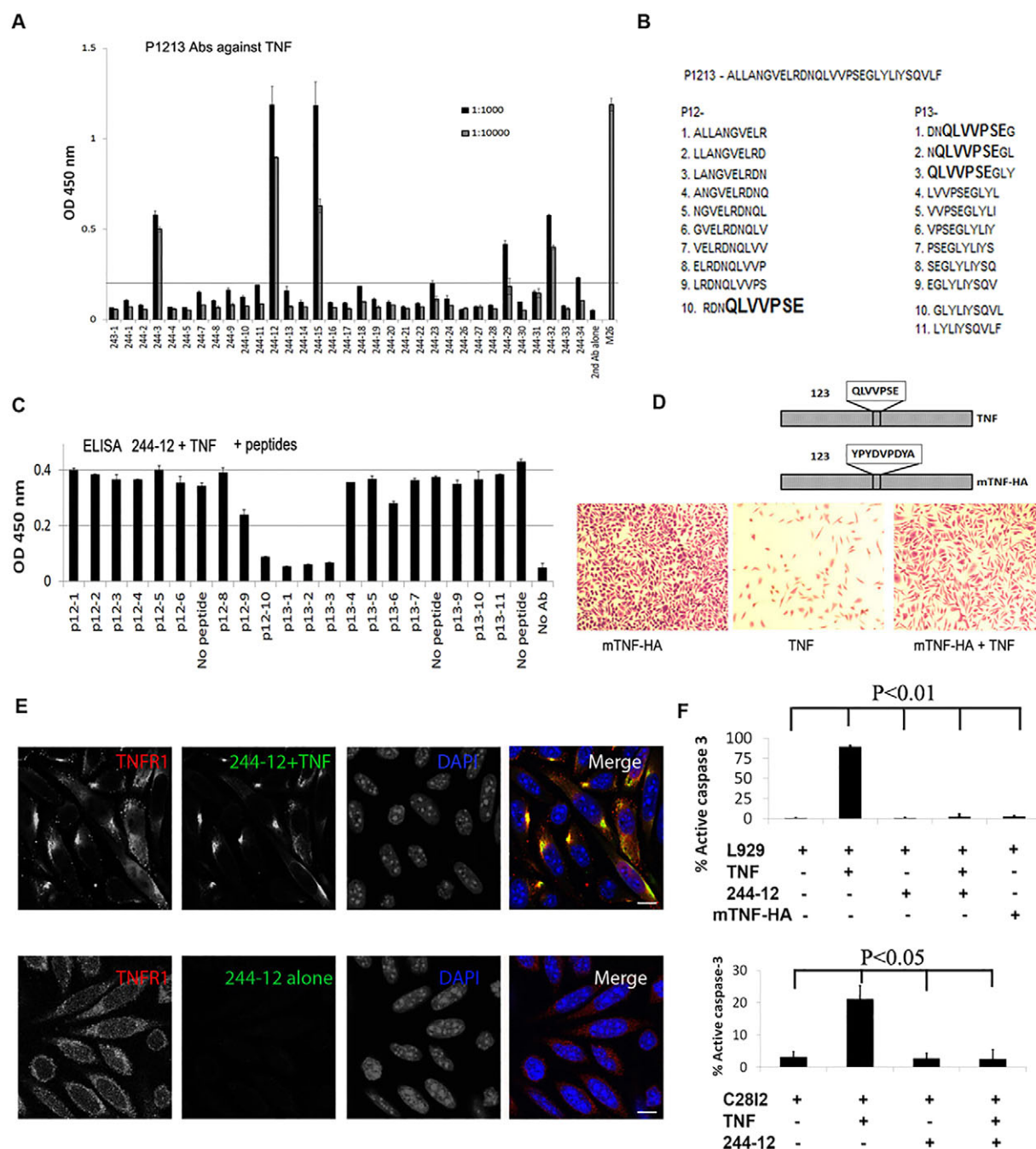


Fig. 6. Apoptosis induced by TNF is due to the function of P1213. (A–C) Screening peptide-targeted mAbs for the binding to TNF. (A) ELISA was used to screen 33 P1213-specific monoclonal antibodies for binding to TNF. (B) A series of 10-mer overlapping peptides comprising the whole P1213 sequence. These peptides are ten amino acids long and overlapped with adjacent peptides by a nine amino acids. (C) Mapping the epitope of mAb 244-12 for binding to TNF. Inhibition ELISA test of mAb 244-12 binding to TNF was performed by adding each of the 10-mer overlapping peptides mentioned above to the incubation reaction of mAb 244-12 and TNF. (D) Replacement of the mAb 244-12 binding motif (QLVVPSE) eliminates the TNF killing function. QLVVPSE was replaced by the human influenza HA tag to make mTNF-HA (upper panel). mTNF-HA at 100 µg/ml did not kill L929 cells but competed with wild-type TNF to inhibit its cytotoxicity. L929 cells were cultured with TNF, mTNF-HA or TNF+mTNF-HA overnight, followed by fixing and staining with 0.05% Crystal Violet buffer. (E) Binding of mAb 244-12 to TNF does not affect TNF binding to TNFR1. mAb 244-12 was incubated with TNF for 2 h before adding to the culture of L929 cells. The cells were simultaneously stained with an antibody against TNFR1 conjugated with Alexa-Fluor-568 and an anti-mouse IgG conjugated with Alexa-Fluor-488 (for mAb 244-12) before examination with a confocal microscope. Scale bars: 10 µm. (F) mAb 244-12 (or mTNF-HA) blocks TNF-induced apoptosis in L929 cells and C2812 cells. L929 cells or C2812 chondrocytes were incubated with TNF or mTNF-HA in the presence or absence of mAb 244-12 before the measurement of intracellular active caspase-3. The error bars represent mean±s.d. of three experiments. *P*-values were calculated using Student's *t*-test.

It is important to know whether the apoptosis induced by the whole TNF molecule is due to the sequence corresponding to P1213. We addressed this question using strategies involving a mutant TNF protein and a monoclonal antibody (mAb 244-12) that

binds to a specific epitope within the P1213 region. Mutant TNF competed with wild-type TNF because it inhibited wild-type-TNF-mediated killing when both were present in cell culture (Fig. 6D). Moreover, TNF-induced apoptosis was also inhibited when the

wild-type TNF was replaced with the mutant (Fig. 6F). By binding to TNF, mAb 244-12 does not affect TNF binding to its receptor (Fig. 6E) but blocks the expression of caspase-3 (Fig. 6F). These data strongly suggest that the P1213 region is key to TNF-induced apoptosis. Previous reports have shown that after TNF binding to its receptor, it is degraded into fragments that might initiate the process of cell death within 2–6 h (Kull and Besterman, 1990; Tsujimoto et al., 1985). Our data support this by showing that a specific sequence in linear TNF peptides can directly bind to TRADD to start the process of apoptosis.

Our results suggest that the evolutionarily conserved primary sequences of TNF relate to its original functions in cell death and that secondary structure is important to the more recently evolved function of NF- κ B activation. The primitive molecule has evolved to become sophisticated with diverse and sometimes apparently conflicting functions. The activities we have discerned here for some of its component peptides could go some way to explaining its complex biology. The possibility of using TNF peptides to elicit specific TNF effects raises new hope for potential applications in drug targeting and/or discovery.

MATERIALS AND METHODS

Cells lines, TNF and peptides

L929, Jurkat A3, RIP^{-/-} and I9.2 (caspase-8^{-/-}) cells were purchased from American Type Culture Collection (ATCC, Manassas, VA). I2.1 (FADD^{-/-}) was a gift from L. Zheng (National Institutes of Health, Bethesda, MA). Human C28I2 chondrocytes were provided by Mary B. Goldring (Hospital for Special Surgery, New York City, NY). Human Saos-2 (osteosarcoma) cell line was purchased from Sigma-Aldrich.

TNF was purchased from Immunotools (Friesoythe, Germany). Peptides, whose sequences are shown in Fig. 1A, and their modification (e.g. biotinylation) were synthesized on an automatic APEX 396 using a standard solid phase Fmoc strategy. In some of the validation experiments, peptides (e.g. P12 and P16) were purchased from Proimmune (Oxford, UK).

Mutant TNF-HA (mTNF-HA; where QLVVPSE was replaced with the HA tag YPYDVPDYA, starting at position 123) was synthesized by Invitrogen, and the mutant protein was expressed in *Escherichia coli* and purified as described previously (Loetscher et al., 1993).

Apoptosis and necrosis assay

Cells were incubated overnight (or at the times indicated in the figures) with TNF (Immunotools) or TNF peptides with or without 10 μ M z-VAD-FMK (R&D Systems) or TNFR1 (PeproTech, Rocky Hill, NJ). Cells were then stained using a live–dead cell staining kit (Invitrogen, Paisley, UK), following the manufacturer's instructions. The cells were then fixed with the Cytofix/Cytoperm fixation and permeabilization solution kit (BD Pharmingen), followed by intracellular staining with a FITC-conjugated anti-caspase-3 antibody (BD Pharmingen). Cell data were acquired on a CyAn flow cytometer (Beckman Coulter, Fullerton, CA), and data were analyzed using Flowjo (Tree Star Inc., Ashland, Oregon).

TNF cytotoxicity assay

Adherent L929 cells (100 μ l, 4×10^5 /ml) were incubated with TNF or peptides, with or without the presence of actinomycin D (8 μ g/ml) (Sigma-Aldrich) overnight at 37°C under 5% CO₂. After aspiration of all the supernatant, 50 μ l of 0.05% Crystal Violet was added to each well to stain the live cells. After rinsing off Crystal Violet, the viability of the attached cells could be determined.

NF- κ B assay

Jurkat A3 cells, which were treated with TNF or their peptides at the indicated time points (Figs 1B and 2A), were harvested and lysed in RIPA lysis buffer (Cell Signaling Technology, Danvers, MA) with protease cocktail inhibitor (Sigma-Aldrich). Cell extracts were then blotted onto nitrocellulose membranes (Amersham Life Science, Little Chalfont, UK),

followed by probing with an antibody against I κ B α (Cell Signaling Technology, Danvers, MA, USA) and detection using chemiluminescence.

Transmission electron microscopy

In some experiments, after the incubation of cells with peptides, the cells were processed for transmission electron microscopy analysis (a service provided by Oxford Brooks University).

Nuclear DNA fragmentation

Some cells were stained with DAPI (Vector Laboratories), in addition to analysis using the live–dead staining kit and anti-caspase-3 antibody (BD Biosciences). Cells were then observed under a fluorescent microscope.

siRNA knockdown of TNFR1

Five million Jurkat A3 cells were mixed either with 240 pmol of validated siRNA against TNFR1 (Life Technologies; catalog number 4390824) or with a negative siRNA control (Life Technologies; catalog number 4390843) duplexes. The mixture was transferred to a 0.4-cm cuvette, and cells were electroporated under 260 V, 720 Ω and 1050 μ F at room temperature using nucleofactor (Amaxa, Cologne, Germany). After electroporation, the cells were resuspended in 6 ml of cell culture medium and placed in a 6-well plate. The cells were cultured for 2 days before further treatment with or without P1213 peptides.

Immunoprecipitation and western blotting

For immunoprecipitation, 20 million Jurkat A3 cells were stimulated with 100 ng/ml TNF or 100 μ M P1213 for 10 min or 2 h at 37°C. The cells were washed with cold PBS and lysed with 1 ml RIPA buffer (NEB, Hertfordshire, UK) containing protease inhibitor cocktail (Roche) on ice. Homogenized samples were microcentrifuged at full speed for 15 min at 4°C. The supernatants, pre-cleared by incubation with 50 μ l Protein-G Sepharose beads, were subjected to immunoprecipitation overnight at 4°C using Protein-G beads coupled with 15 μ g of antibody against TRADD (BD Biosciences). The immunoprecipitated beads were washed five times with cold lysis buffer and subjected to SDS-PAGE. The separated proteins were transferred onto nitrocellulose membrane and probed with the following antibodies: mouse anti-TRADD, rabbit anti-TNFR1 (Abcam), mouse anti-RIP1 (BD Biosciences) and rabbit anti-FADD (Cell Signaling) antibodies.

Confocal microscopy

Cells that had been grown on cover slips were stimulated under one of the following conditions: biotinylated TNF or peptides for 10 min at 37°C, or pre-mixed TNF+mAb 244-12 or mAb 244-12 alone for 30 min on ice. The cells were fixed in 3% paraformaldehyde for 10 min at room temperature. After permeabilization (0.5% Triton X-100 in PBS), the cells were blocked with phosphate-buffered gelatin and 1% FCS for 30 min, and incubated with appropriate primary antibodies for 1 h at room temperature. The cells were washed and incubated for another hour with the appropriate secondary antibodies conjugated with either Alexa-Fluor-488 or Alexa-Fluor-568 (Invitrogen). Nuclei were counter stained with DAPI (Sigma-Aldrich). The cells were imaged using a ZEISS 780 inverted confocal laser scanning microscope (ZEISS, Cambridge, UK) and analyzed by using Zen software.

Peptide structure – circular dichroism

Circular dichroism spectra were acquired on a specially adapted Jasco J720 spectrometer, with a bespoke thermostatic cell holder that maintained a temperature of 20.0 \pm 0.1°C in the spectroscopic cell and that was flushed with copious evaporated N₂ to improve performance in the far-UV wavelength region.

Circular dichroism spectroscopy analysis of P16 in liposomes

Circular dichroism spectra were recorded between 190 and 260 nm on a Jasco J-850 spectropolarimeter equipped with a temperature-controlled incubator at 25°C using 0.1-mm optical path length quartz cells. Circular dichroism spectra of P16 (50 μ M) were measured in aqueous buffer solution (50 mM KH₂PO₄–K₂HPO₄, pH 7.2) or in the presence of 2.5 mM

liposomes. The results are expressed as the mean residue ellipticity $[\theta]$ in units of degree $\text{cm}^2 \text{dmol}^{-1}$.

Liposome preparation

Liposomes comprising POPC and palmitoyl-oleoyl-phosphatidylethanolamine (POPE; POPC:POPE) (1:1) and POPC:POPS (1:1) were prepared by sonication. Briefly, POPC, POPE and POPS in chloroform were mixed at the desired molar ratios. Chloroform was removed using a stream of argon at room temperature to form a lipid film. The lipid film was then placed in a vacuum desiccator overnight to remove residual chloroform. The lipid film was re-suspended in 50 mM KH_2PO_4 – K_2HPO_4 , pH 7.2 at a concentration of 2.5 mg/ml with vigorous vortexing and then sonicated at 4°C using a probe sonicator until a clear lipid suspension was obtained.

Dynamic light scattering

The size of P16 was represented by its hydrodynamic radius (nm), measured by dynamic light scattering under hydrophilic or hydrophobic conditions.

Briefly, the peptides at 1 mg/ml were measured using the Viscotek 802 DLS from Malvern. Peptide samples in DMSO (50 mg/ml) were diluted into 50 mM KH_2PO_4 /K₂HPO₄, pH 7.2 or 40% TFA with 60% 50 mM KH_2PO_4 /K₂HPO₄ and spun at 12,000 *g* for 10 min before loading 10 μl into the cuvettes. Fifty scans of 5 s were acquired for each sample at 25°C. The data was processed using default settings in the Wyatt software, corrected for solvent signal.

Effect of peptides on cell membrane

Lysis of red blood cells

RBCs were separated and incubated with or without the presence of peptides or sterile water at 37°C under 5% CO_2 overnight. The hemoglobin in the supernatant was measured at OD_{490 nm} with a Wallac Victor² 1420 multilabel counter (PerkinElmer, Massachusetts, MA, USA).

Lysis of lipid membranes

First, the encapsulated membrane-impermeable fluorescent indicators were prepared as follows – an aliquot of 10-mM membrane-impermeable copper-ion-sensitive fluorescent dye Phen Green SK (Invitrogen) was added to the liposome re-suspension to a final concentration of 200 μM . The samples were sonicated for 10 s and subjected to one cycle of freeze–thaw (liquid nitrogen and room temperature), followed by an additional 10-s sonication. The untrapped indicator exterior to the liposomes was removed using an Econo-Pac 10 DG desalting column pre-equilibrated with 50 mM KH_2PO_4 /K₂HPO₄, pH 7.2, 5 μM CuCl₂. The indicator-loaded proteoliposomes were eluted in the void fraction.

The liposome membrane disruption assay was performed on the FLUOstar Omega plate reader (BMG Labtech). The liposome leakage reactions were initiated by the injection of 10 μl of 500 μM of P16. The quenching of fluorescence emission (the changes in Phen Green SK fluorescence monitored by exciting the samples at 490 nm and collecting emission data at 515 nm) was measured as a function of leakage.

Generation of peptide-P1213-specific monoclonal antibodies

Female BALB/c mice (8 weeks old) were immunized with 30 μg of peptide P1213 conjugated with bovine serum albumin (P1213–BSA) (Generon, Maidenhead, UK) in a complete Freund's adjuvant by subcutaneous injection. The immunization was boosted 4 weeks later with 30 μg of P1213–BSA mixed with an incomplete Freund's adjuvant by subcutaneous injection. The third immunization was performed 3 weeks later with 30 μg of P1213–BSA in PBS by intraperitoneal injection. The titer of anti-P1213 antibodies in sera was monitored 10 days after the last immunization using an indirect ELISA. P1213 was conjugated with keyhole limpet hemocyanin (P1213–KLH) (Generon) for the screening of mAbs. Subsequently, one immunized mouse with the highest sera titer of anti-P1213 antibodies was further boosted with 30 μg of P1213–BSA in PBS by intraperitoneal injection. Three days later, splenocytes from the boosted mouse and SP2/0 myeloma cells were fused in the presence of 50% polyethylene glycol (PEG; molecular mass 4000, Merck, Darmstadt, Germany). The positive hybrids were selected using an indirect ELISA with a coating of P1213–KLH and

then sub-cloned three times using the limiting dilution method. Monoclonal antibodies targeting the peptide P1516 were made in the same way as described above using P1516 as the antigen.

ELISA

Purified avidin (2 $\mu\text{g}/\text{ml}$, Sigma-Aldrich) or TNF (2 $\mu\text{g}/\text{ml}$) were coated onto flat-bottomed 96-well microtiter plates (Nunc, Denmark) in PBS overnight at 4°C. The wells were blocked with 5% BSA for 1 h at room temperature before the addition of biotinylated peptides (2 $\mu\text{g}/\text{ml}$) or TNF (2 $\mu\text{g}/\text{ml}$). This followed by incubating with soluble TNFR1 (5 $\mu\text{g}/\text{ml}$) at room temperature for 1 h. The binding was detected by using HRP-conjugated anti-TNFR1 antibodies.

In another experiment, TNF-coated- and BSA-blocked plates were incubated at room temperature for 1 h with diluted anti-P1213 monoclonal antibodies (1:1000 or 1:10,000) and either further incubated with 10-mer overlapping peptides (Fig. 6C) or directly detected with HRP-conjugated anti-mouse IgG (Fig. 6A). After washing, the plates were developed by adding 100 μl of tetramethylbenzidine substrate solution. The reaction was stopped, and the absorbance at 450 nm was measured using a spectrometer.

Surface plasmon resonance experiments

Binding experiments were performed using surface plasmon resonance with the Biacore[®] 3000 instrument (GE Healthcare). All analyses were performed at 37°C. Analyses of the interaction between TNFR1 and TNFR2 and its ligands (TNF, P1213 and P16) were performed in HBS-EP buffer [0.01 M HEPES, pH 7.4, 0.15 M NaCl, 0.005% (v/v) surfactant P20]. To determine the binding responses of TNFR1 and TNFR2 for their ligands, TNF, P1213 and P16 were directly immobilized onto the dextran matrix of research-grade CM5 sensor chips (GE Healthcare) by amine coupling using the manufacturer's kit (GE Healthcare) with an activation time of 5 min, resulting in immobilization levels of 1000–10,000 response units, and an inactivation time of 5 min. The analytes, 5.3 μM TNFR1 and 5.4 μM TNFR2, were then subsequently injected over flow cells containing the immobilized proteins simultaneously.

Acknowledgements

We thank Dr L. Zheng for I2.1 cells and Dr Mary B. Goldring for human C2812 chondrocytes. We are grateful to Dr Robert Carlisle for his discussion of the project, Dr Suet Lin Chia (University of Oxford, UK) for providing the HT29 cell line and helping with confocal microscope, and Dr Eugene Chang for his critical reading of this article.

Competing interests

S.J., W.L., S.Y. and Z.Y. have filed patents as a result of this project.

Author contributions

S.J. and L.W.S. designed and wrote the manuscript; W.L. and Q.C. performed most of the experiments; S.Y. carried out some fluorescence microscopy experiments; X.X., Z.Y. and G.T. made peptides and performed peptide circular dichroism spectroscopy; Y.L. performed bioinformatic analyses; B.J. and C.S. made monoclonal antibodies.

Funding

This work is supported by The Mary Kinross Charitable Trust. The funder had no role in study design, data collection and analysis, decision to publish, or preparation of the manuscript.

Supplementary information

Supplementary information available online at <http://jcs.biologists.org/lookup/suppl/doi:10.1242/jcs.175463/-/DC1>

References

- Baena, A., Mootnick, A. R., Falvo, J. V., Tsytsykova, A. V., Ligeiro, F., Diop, O. M., Brieva, C., Gagneux, P., O'Brien, S. J., Ryder, O. A. et al. (2007). Primate TNF promoters reveal markers of phylogeny and evolution of innate immunity. *PLoS ONE* 2, e621.
- Bejerano, G., Pheasant, M., Makunin, I., Stephen, S., Kent, W. J., Mattick, J. S. and Haussler, D. (2004). Ultraconserved elements in the human genome. *Science* 304, 1321–1325.
- Berghe, T. V., Vanlangenakker, N., Parthoens, E., Deckers, W., Devos, M., Festjens, N., Guerin, C. J., Brunk, U. T., Declercq, W. and Vandenabeele, P.

- (2010). Necroptosis, necrosis and secondary necrosis converge on similar cellular disintegration features. *Cell Death Differ.* **17**, 922–930.
- Chan, F. K.-M., Shisler, J., Bixby, J. G., Felices, M., Zheng, L., Appel, M., Orenstein, J., Moss, B. and Lenardo, M. J. (2003). A role for tumor necrosis factor receptor-2 and receptor-interacting protein in programmed necrosis and antiviral responses. *J. Biol. Chem.* **278**, 51613–51621.
- Declercq, W., Vanden Berghe, T. and Vandenabeele, P. (2009). RIP kinases at the crossroads of cell death and survival. *Cell* **138**, 229–232.
- Eck, M. J. and Sprang, S. R. (1989). The structure of tumor necrosis factor- α at 2.6 Å resolution. Implications for receptor binding. *J. Biol. Chem.* **264**, 17595–17605.
- Feldmann, M. (2009). Translating molecular insights in autoimmunity into effective therapy. *Annu. Rev. Immunol.* **27**, 1–27.
- Fernandes, H. P., Cesar, C. L. and Barjas-Castro, M. d. L. (2011). Electrical properties of the red blood cell membrane and immunohematological investigation. *Rev. Bras. Hematol. Hemoter.* **33**, 297–301.
- Galluzzi, L. and Kroemer, G. (2008). Necroptosis: a specialized pathway of programmed necrosis. *Cell* **135**, 1161–1163.
- Ghosh, S., May, M. J. and Kopp, E. B. (1998). NF- κ B and Rel proteins: evolutionarily conserved mediators of immune responses. *Annu. Rev. Immunol.* **16**, 225–260.
- Greenfield, N. J. (2007). Analysis of the kinetics of folding of proteins and peptides using circular dichroism. *Nat. Protoc.* **1**, 2891–2899.
- He, S., Wang, L., Miao, L., Wang, T., Du, F., Zhao, L. and Wang, X. (2009). Receptor interacting protein kinase-3 determines cellular necrotic response to TNF- α . *Cell* **137**, 1100–1111.
- Hehlgans, T. and Pfeffer, K. (2005). The intriguing biology of the tumour necrosis factor/tumour necrosis factor receptor superfamily: players, rules and the games. *Immunology* **115**, 1–20.
- Hilchie, A. L., Doucette, C. D., Pinto, D. M., Patrzykat, A., Douglas, S. and Hoskin, D. W. (2011). Pleurocidin-family cationic antimicrobial peptides are cytolytic for breast carcinoma cells and prevent growth of tumor xenografts. *Breast Cancer Res.* **13**, R102.
- Hitomi, J., Christofferson, D. E., Ng, A., Yao, J., Degterev, A., Xavier, R. J. and Yuan, J. (2008). Identification of a molecular signaling network that regulates a cellular necrotic cell death pathway. *Cell* **135**, 1311–1323.
- Hogan, M. M. and Vogel, S. N. (2001). Measurement of tumor necrosis factor α and β . *Curr. Protoc. Immunol.* Chapter 6, Unit 6 10.
- Kull, F. C., Jr and Besterman, J. M. (1990). Drug-induced alterations of tumor necrosis factor-mediated cytotoxicity: discrimination of early versus late stage action. *J. Cell. Biochem.* **42**, 1–12.
- Loetscher, H., Stueber, D., Banner, D., Mackay, F. and Lesslauer, W. (1993). Human tumor necrosis factor α (TNF α) mutants with exclusive specificity for the 55-kDa or 75-kDa TNF receptors. *J. Biol. Chem.* **268**, 26350–26357.
- Martin, E. M., Remke, A., Pfeifer, E., Polz, J., Pietryga-Krieger, A., Steffens-Weber, D., Freudenberg, M. A., Mostböck, S. and Mannel, D. N. (2014). TNFR2 maintains adequate IL-12 production by dendritic cells in inflammatory responses by regulating endogenous TNF levels. *Innate Immun.* **20**, 712–720.
- Micheau, O. and Tschopp, J. (2003). Induction of TNF receptor I-mediated apoptosis via two sequential signaling complexes. *Cell* **114**, 181–190.
- Peschel, A. and Sahl, H.-G. (2006). The co-evolution of host cationic antimicrobial peptides and microbial resistance. *Nat. Rev. Microbiol.* **4**, 529–536.
- Quistad, S. D., Stotland, A., Barott, K. L., Smurthwaite, C. A., Hilton, B. J., Grasis, J. A., Wolkowicz, R. and Rohwer, F. L. (2014). Evolution of TNF-induced apoptosis reveals 550 My of functional conservation. *Proc. Natl. Acad. Sci. USA* **111**, 9567–9572.
- Riedl, S., Zwegytick, D. and Lohner, K. (2011). Membrane-active host defense peptides—challenges and perspectives for the development of novel anticancer drugs. *Chem. Phys. Lipids* **164**, 766–781.
- Tsujiimoto, M., Yip, Y. K. and Vilcek, J. (1985). Tumor necrosis factor: specific binding and internalization in sensitive and resistant cells. *Proc. Natl. Acad. Sci. USA* **82**, 7626–7630.
- Van Noorden, C. J. F. (2001). The history of Z-VAD-FMK, a tool for understanding the significance of caspase inhibition. *Acta Histochem.* **103**, 241–251.
- Vandenabeele, P., Galluzzi, L., Vanden Berghe, T. and Kroemer, G. (2010). Molecular mechanisms of necroptosis: an ordered cellular explosion. *Nat. Rev. Mol. Cell Biol.* **11**, 700–714.
- Varfolomeev, E. E. and Ashkenazi, A. (2004). Tumor necrosis factor: an apoptosis JuNKie?. *Cell* **116**, 491–497.
- Vercammen, D., Beyaert, R., Denecker, G., Goossens, V., Van Loo, G., Declercq, W., Grooten, J., Fiers, W. and Vandenabeele, P. (1998). Inhibition of caspases increases the sensitivity of L929 cells to necrosis mediated by tumor necrosis factor. *J. Exp. Med.* **187**, 1477–1485.
- Wiens, G. D. and Glenney, G. W. (2011). Origin and evolution of TNF and TNF receptor superfamilies. *Dev. Comp. Immunol.* **35**, 1324–1335.
- Wong, W. W.-L., Gentle, I. E., Nachbur, U., Anderton, H., Vaux, D. L. and Silke, J. (2010). RIPK1 is not essential for TNFR1-induced activation of NF- κ B. *Cell Death Differ.* **17**, 482–487.
- Wu, Y.-T., Tan, H.-L., Huang, Q., Sun, X.-J., Zhu, X. and Shen, H.-M. (2011). zVAD-induced necroptosis in L929 cells depends on autocrine production of TNF α mediated by the PKC-MAPKs-AP-1 pathway. *Cell Death Differ.* **18**, 26–37.
- Zhang, D.-W., Shao, J., Lin, J., Zhang, N., Lu, B.-J., Lin, S.-C., Dong, M.-Q. and Han, J. (2009). RIP3, an energy metabolism regulator that switches TNF-induced cell death from apoptosis to necrosis. *Science* **325**, 332–336.

Special Issue on 3D Cell Biology
Call for papers

Submission deadline: January 16th, 2016

Journal of
Cell Science